Modelling Dysregulated Na^+ Absorption in Airway Epithelial Cells with Mucosal Nystatin Treatment

Alessandra Livraghi[1], Marcus Mall[2], Anthony M. Paradiso[1†], Richard C. Boucher[1,3], and Carla M. Pedrosa Ribeiro[1,3]

[1]Cystic Fibrosis/Pulmonary Research and Treatment Center, and [3]Department of Medicine, The University of North Carolina at Chapel Hill, Chapel Hill, North Carolina; and [2]Department of Pediatrics III, Pediatric Pulmonology and Cystic Fibrosis Center, University of Heidelberg, Heidelberg, Germany

In cystic fibrosis (CF), the absence of functional CFTR leads to dysregulated Na^+ absorption across airway epithelia. We established an *in vitro* model of dysregulated Na^+ absorption by treating polarized normal human bronchial epithelial cells (HBEs) with nystatin (Nys), a polyene antibiotic that enables monovalent cations to permeate biological membranes. Acute mucosal Nys produced a rapid increase in short circuit current (I_{sc}) that reflected increased transepithelial Na^+ absorption and required Na^+/K^+ATPase activity. The acute increase in I_{sc} was associated with increased mucosal liquid absorption. Prolonged mucosal Nys treatment resulted in sustained Na^+ hyperabsorption, associated with increased mucosal liquid absorption in comparison with naïve (nontreated, kept under air–liquid interface conditions) or vehicle-treated cultures. Nys treatment was not toxic. Increased lactate accumulation in Nys-treated culture media suggested a higher metabolic rate associated with the higher energy demand for Na^+ transport. After chronic Nys treatment, the increased I_{sc} was rapidly lost when the cultures were mounted in Ussing chambers, indicating that Nys could be rapidly removed from the apical membrane. Importantly, chronic Nys treatment promoted sustained mucosal liquid depletion and caused mucus dehydration, compaction, and adhesion to the apical surface of Nys-treated cultures. We conclude that mucosal Nys treatment of HBEs provides a simple *in vitro* model to recapitulate the Na^+ and volume hyperabsorptive features of CF airway epithelia.

Keywords: nystatin; Na^+ hyperabsorption; airway surface liquid dehydration; mucus adherence; cystic fibrosis

In cystic fibrosis (CF) airways, the absence of functional cystic fibrosis transmembrane conductance regulator (CFTR) protein results in deficient cAMP-dependent Cl^- secretion and dysregulated Na^+ transport (1). This ion transport imbalance leads to depletion of the airway surface liquid (ASL) volume and impairment in mucus clearance (2), which results in airway obstruction and increased susceptibility to infection and inflammation (3). The link among Na^+ hyperabsorption, ASL dehydration, and the onset of CF lung disease has been strongly supported by the airway phenotype of the recently generated *Scnn1b*-transgenic mouse, in which airway-targeted overexpression of the epithelial Na^+ channel β subunit (βENaC, encoded by the *Scnn1b* gene) resulted in increased epithelial Na^+ absorption, ASL depletion, impaired mucociliary clearance, and airway inflammation (4).

CLINICAL RELEVANCE

Our model recapitulates two key features of cystic fibrosis (CF) airways: abnormal Na^+ transport and cell surface accumulation of dehydrated mucus. This model may be used to characterize interactions in a milieu resembling CF airways.

In vitro cultures of human airway epithelial cells have been widely used to study fundamental aspects of CF and other lung diseases (5), as these cultures recapitulate many features of the native respiratory epithelia (6, 7). Although lungs explanted from patients with CF during transplantation represent a valuable source of primary CF cells for culture, the availability of such specimens is limited. Moreover, recent studies have shown that at least the inflammatory phenotype of primary cultures of CF airway changes in short-term (6–11 d) versus long-term well-differentiated (30–40 d) cultures (8). To investigate the specific contribution of epithelial Na^+ hyperabsorption *per se* to the development of CF lung disease, there is a need to consistently reproduce the Na^+ hyperabsorptive phenotype of CF airway epithelia in an *in vitro* model.

In the present study, we sought to recapitulate the CF-like Na^+ hyperabsorptive phenotype in primary cultures of normal human bronchial epithelial cells (HBEs) by exploiting the pore-forming capacity of the polyene antibiotic nystatin (Nys), which selectively enables monovalent cations to permeate sterol-containing membranes. Nys, like another polyene antibiotic amphotericin B, forms monovalent cation-selective pores with a permeability sequence of $Rb^+ > K^+ > Na^+ > Li^+$, identical to the size order of the hydrated ions. Nys has been widely used in perforated patch recordings to gain electrical access to the cytoplasm while blocking the diffusion of cellular constituents into the patch pipette (9). To establish an *in vitro* model of transepithelial Na^+ hyperabsorption, we first characterized the response of polarized HBE cultures to acute mucosal Nys challenge. Next, we evaluated the effect of prolonged Nys treatment on HBEs by comparing Nys-treated cultures with nontreated (naïve) and vehicle-treated (KBR) cultures. We studied the bioelectric properties, changes in the expression of Na^+ transport mediators, toxicity, apical volume absorption, and effect on mucosal secretions elicited by Nys treatment.

MATERIALS AND METHODS

Cell Culture

Primary normal HBEs were provided by the UNC CF Center Tissue Core and obtained under the auspices of protocols approved by the Institutional Committee for the Protection of the Rights of Human

(*Received in original form May 17, 2007 and in final form October 12, 2007*)

†Deceased.

This work was supported by contract grant sponsors: Cystic Fibrosis Foundation, the National Institutes of Health, and Deutsche Forschungsgemeinschaft (DFG). Contract grant numbers: CF Foundation CFFRIBEIRO0Z0 and CFFRIBEIRO0G0 to C.M.P.R; NIH P01 HL034322 (PPG), NIH P50 HL060280 (SCOR), NIH P50 HL084934 (SCCOR), NIH P30 DK065988 (MTCC), and CF Foundation R026-CR02 (CFF RDP) to R.C.B; and DFG MA 2081/2–1 to M.M.

Correspondence and requests for reprints should be addressed to Alessandra Livraghi, Ph.D., University of North Carolina at Chapel Hill, Cystic Fibrosis/Pulmonary Research and Treatment Center, CB#7248 Thurston Bowles Bldg., Room # 6029, Chapel Hill, NC 27599. E-mail: alessandra_livraghi@med.unc.edu

This article has an online supplement, which is accessible from this issue's table of contents at www.atsjournals.org

Am J Respir Cell Mol Biol Vol 38. pp 423–434, 2008
Originally Published in Press as DOI: 10.1165/rcmb.2007-0177OC on November 7, 2007
Internet address: www.atsjournals.org

Subjects. HBEs were obtained from freshly excised main stem or lobar bronchi by protease digestion, directly seeded on 12-mm Transwell Col membranes (Corning-Costar Corp., Cambridge, MA), maintained in modified bronchial epithelial growth medium under air–liquid interface conditions as previously described (10), and studied when transepithelial resistance (R_T) was $\geq 300\ \Omega \cdot cm^2$.

Ussing Chamber Measurements

HBEs were plated on 12-mm Snapwell-Clear membranes (Corning-Costar) pre-coated with human placenta type IV collagen (0.74 mg/ml; Sigma-Aldrich, St. Louis, MO) in modified bronchial epithelial growth medium, as described above (10). For acute Nys treatment experiments, naïve cultures were mounted in Ussing chambers and bilaterally bathed in Krebs-bicarbonate Ringer (KBR, composition in mM: 140 Na^+, 120 Cl^-, 5.2 K^+, 25 HCO_3, 2.4 HPO_4, 0.4 H_2PO_4, 1.2 Ca^{2+}, 1.2 Mg^{2+}, 5 glucose, pH 7.4) bubbled with 95% O_2–5% CO_2. Other bathing solutions included: bilateral Cl^- free KBR, as KBR except all Cl^- was substituted by gluconate; bilateral HCO_3^- free KBR, as KBR except HCO_3 was substituted with 1 mM HEPES, 1mM acetazolamide was added to inhibit cellular bicarbonate production, and the solution was bubbled with 100% O_2; and mucosal high K^+ KBR, as KBR except K^+ was increased to 100 mM and Na^+ reduced to 45 mM. Bioelectric measurements were performed under short circuit current (I_{sc}) conditions at 37°C. Changes in I_{sc} were measured in response to amiloride (100 μM, mucosal), Nys (40 μM, mucosal), ouabain (1 mM, serosal), or bumetanide (100 μM, serosal). For chronic Nys treatment experiments, the transepithelial voltage (V_T) and R_T of naïve, KBR-, and Nys-treated cultures were measured with epithelial Voltohmeter (EVOM; World Precision Instruments, Sarasota, FL) as described in detail below. On the fourth day of treatment, the cultures were mounted in Ussing chambers and bilaterally bathed in KBR. Changes in I_{sc} were measured in response to acute addition of Nys (40 μM, mucosal).

Perfusion Ussing Chamber Measurements

HBE cells were plated on porous Transwell Col filters (insert diameter ~ 2–3 mm), as previously described (11). After confluence was achieved, polarized monolayers were mounted in a modified miniature Ussing chamber connected to a perfusion system that allows rapid (flow rate 3–5 ml/min, half-time for solution exchange < 3 s) and independent change of the solutions bathing the apical and basolateral surface of the culture. Nys (40 μM in KBR) or KBR alone were used as mucosal perfusates, while KBR was the serosal perfusate in all experiments. For bioelectric measurements, V_T was monitored by a voltage clamp/pulse generator and the signal recorded. All experiments were performed under open circuit conditions. To calculate the equivalent current from changes in V_T in response to Nys-challenge, a 1-second current pulse (1 μA) was delivered across the tissue every 5 seconds. Chord resistances were calculated at different time points based on the magnitude change in the deflection of V_T, and the equivalent current (I_{eq}) was calculated using Ohm's law, according to a method described by Paradiso and coworkers (11).

Volume Absorption Measurements

We performed two types of ASL measurements. First, "thin-film" measurements of Texas Red–labeled ASL volume (steady-state and kinetic) were performed with the laser confocal microscopy technique (described in detail in Ref. 12), using a Zeiss Meta Laser Scanning confocal microscope (Zeiss, Jena, Germany), with a C-Apochromat 40×/1.2 NA water immersion lens (objective working distance 0.29 mm). For steady-state measurement of ASL height, at t = 0, 10 μl of Texas Red–labeled (2 mg/ml) Hepes-buffered saline solution (HBSS, in mM: 130 NaCl; 5 KCl; 1.3 $MgCl_2 \cdot 6H_2O$; 1.3 $CaCl_2$; 5 glucose, and 10 HEPES salt-free, pH 7.4) was applied to the mucosal surface and the excess volume aspirated with a Pasteur pipette to set "thin film conditions" (~ 1 μl) and avoid meniscus-derived artifacts. Due to the fast rate of volume absorption observed in preliminary experiments in the presence of Nys, for volume absorption kinetic studies 10 μl of Texas Red dextran–labeled volume, in the presence or absence of Nys, were layered on the mucosal surface of the cultures and imaged at different time points (5 min, 30 min, 1 h, 6 h, and 24 h). For all studies, 100 μl perfluorocarbon (PFC) was added mucosally before imaging to prevent evaporation of the ASL. To measure the average ASL height, five randomly selected fields in predetermined areas on the culture (one central, four circumferential) were scanned in the XZ mode. Images were then analyzed using the Zeiss LSM 5 Image software, by measuring ASL height with the calibrated line drawing tool in three randomly selected points for each image. ASL height data ($n = 3$ transwells/condition from two to three different donors) were then averaged for each condition and time point.

Second, during chronic Nys treatment, macroscopic volume absorption was measured by quantifying the mucosal liquid still present on the surface of the cultures at 8 and 16 hours after each mucosal application of KBR or KBR+Nys. The residual volume was harvested by gentle suction and its volume measured gravimetrically.

Cell Swelling Measurements

Naïve HBE cultures were bilaterally loaded with 4 μM calcein-AM in Ham's F12 medium for 30 minutes at 37°C, washed with PBS, and imaged in the XZ scanning mode using a Zeiss Meta Laser Scanning confocal microscopy, with a C-Apochromat 40×/1.2 NA water immersion lens. After recording the baseline epithelial height at t = 0, 200 μl HBSS with or without 40 μM Nys were added to the mucosal surface and sequential scans were taken every 5 minutes. Cell swelling was monitored for up to 45 minutes.

Chronic Nys Treatment

A 40 mM sterile stock solution of Nys (Sigma) was prepared in dimethyl sulfoxide (DMSO), aliquoted, and frozen at −20°C. A new stock solution was prepared every 2 to 3 weeks. A 1:1,000 dilution was prepared in KBR before each addition and vortexed. Alternatively, a commercially available Nys suspension in Dulbecco's Phosphate Buffered Saline (2 mg/ml, 10,000 units/ml, cell culture tested, endotoxin tested, LPS< 0.016 U/ml; Sigma) was used as stock solution, with comparable results. The bioelectric properties of the HBE cultures during chronic Nys treatment were assessed by measuring the V_T and R_T with an EVOM. We recorded the instantaneous V_T and R_T values after addition of 500 μl KBR to the apical side of the culture to create a mucosal electrolyte bath suitable for measurement. Excess KBR was carefully removed from the mucosal surface by aspiration after each measurement. The equivalent current (I_{eq}) was calculated from the V_T and R_T values according to the Ohm's law. After the initial (t = 0) measurement of V_T and R_T, 120 μl of KBR (vehicle, either KBR alone or KBR + 0.1% DMSO, whenever the Nys 1,000× stock solution in DMSO was used) or KBR + 40 μM Nys (Nys) were mucosally applied to the cultures. KBR or Nys were mucosally applied twice a day, with an 8-hour interval between the first and the second application. Naïve cultures were kept under air–liquid interface conditions throughout the duration of the experiment. Measurements of V_T and R_T were performed as described above, every 24 hours thereafter. In Nys-treated cultures, EVOM V_T readings reached a peak immediately after addition of 500 μl mucosal KBR and quickly declined afterwards. This phenomenon has been also described in toad bladder A6 cells in a similar experimental setting (13). The values reported in Figure 5 correspond to the peak values. A typical chronic Nys treatment protocol lasted 96 hours. The serosal media of all cultures were replaced every 24 hours.

Cell Toxicity Assays

To assess cell toxicity, lactate dehydrogenase activity (LDH) was measured by a colorimetric assay in samples of serosal media collected after 96 hours of chronic Nys treatment. Cell viability after chronic Nys treatment was also assessed through the LIVE/DEAD Viability/Cytotoxicity assay (Invitrogen, Carlsbad, CA). Briefly, after 96 hours of treatment, naive, KBR-, and Nys-treated cultures were incubated with 3 μM calcein (the green fluorescence of calcein depends on intracellular esterase activity, which is present only in viable cells) and 4 μM ethidium homodimer-1 (EthD-1; this dye is excluded by the intact plasma membrane of live cells, whereas it enters cells with damaged membranes and, upon binding to nucleic acids, undergoes a 40-fold enhancement of fluorescence), and imaged by confocal microscopy in XZ scanning mode, as described above.

Lactate Concentration Assays

Twenty microliters of serosal media from naïve, KBR-, and Nys-treated cultures were collected at selected time points over the last 24 hours of

the chronic Nys treatment protocol (i.e., 72, 73, 75, 78, 80, and 96 hours). Secreted lactate was measured by an enzymatic colorimetric assay (Sigma).

Quantitative Real-Time PCR Analysis of mRNA Abundance

RNA extraction (four Transwells/condition, two donor codes) was performed using the RNeasy mini kit (Qiagen, Valencia, CA). Total RNA was reverse transcribed into cDNA. Quantification of the mRNA levels for different transporters was carried on by RT-PCR, using Sybr Green detection in LightCycler (Roche Diagnostics, Basel, Switzerland) according to the manufacturer's instructions. Specific sequences were amplified using the following custom made (MWG Biotech, High Point, NC) primers. Na^+/K^+ATPase α_1 subunit: 5′GGA GCT GCT CTG TGC TTT TC; 3′GCC CTT TTT GCC CTT TTT AT; Na^+/K^+ATPase β_1 subunit: 5′AAG GAG TTT CTG GGC AGG AC; 3′GCC ACT CGG TCC TGA TAT GT; FYXD5: 5′GAG CCC CAG ATG CAG TCT AC; 3′GGG TCT GTC TGG ACG TCT GT; ENaC α-subunit: 5′TGG CAT GAT GTA CTG GCA AT; 3′AGC TCC TCC AGC TCC TCT TT; ENaC β-subunit: 5′TCC GTA GGC TTC AAG ACC AT; 3′CAA TAA GGA CCA GGG GTG TG; ENaC γ-subunit: 5′ATC GAG TCC AAG CAA GTG GT; 3′GTG GTG GAA AAG CGT GAA AT; NKCC1: 5′AAT GAT GGC CAC TGT TGT GA; 3′TTT CTG CAA ATC CAA CCA CA. Results were normalized on the expression levels of GAPDH mRNA, primers 5′GGA GGT GAA GGT CGG AGT CA; 3′GAT CTC GCT CCT GGA AGA TG.

Immunofluorescence Analysis of α_1Na^+/K^+ATPase Subunit

Immunofluorescent detection of the α_1Na^+/K^+ATPase subunit in HBE cultures was performed using a mouse monoclonal antibody (Upstate Technology, Lake Placid, NY). Sections (4–5 μm thick) were obtained from 4% paraformaldehyde–fixed, paraffin-embedded HBE cultures. Antigen retrieval was performed by boiling the slides for 15 minutes in Antigen Unmasking Solution (Vector Laboratories, Burlingame, CA). Blocking was performed in 10% normal goat serum in PBS, for 1 hour at 37°C. The primary antibody was applied to the sections at a 1:200 dilution in PBS. Mouse IgG_1 (Serotec, Raleigh, NC) was used as isotypic control. The secondary antibody was goat anti-mouse FITC (Jackson Immunoresearch, West Grove, PA), used at 15 μg/ml in PBS and incubated for 30 minutes at room temperature in the dark. Nuclear staining was achieved by incubation with 0.5 μg/ml propidium iodide in PBS for 5 minutes at room temperature. Slides were mounted with Vectashield Hard Mount media (Vector Laboratories) and imaged by confocal microscopy, using a Leica SP2 microscope (Leica, Wetzlar, Germany), with an Apochromat 40×/1.25 NA oil immersion lens, in the XY scanning mode. Images were acquired using identical illumination intensity and detection sensitivity settings. Quantification of the specific fluorescence signal was performed using the Metamorph image analysis software (Molecular Devices, Downington, PA).

Osmium/Perfluorocarbon (OsO_4/PFC) Fixation and AB-PAS Staining

OsO_4/PFC fixation followed by Richardson's staining was performed according to the protocol described in (14). For AB-PAS staining, HBE cultures were bilaterally fixed in 4% paraformaldehyde for 15 minutes at room temperature, washed three times with PBS, processed for inclusion in paraffin, cut, and stained according to the method of Sheehan and Hrapchak (15).

Mucus Wet/Dry Ratio Measurements

HBE cultures were either maintained in naïve conditions (without washing of the apical surface) or treated by adding 50 μl of KBR or KBR + 40 μM Nys once a day for 14 days to allow accumulation of visible mucous material. Mucus samples were removed with forceps and weighed at three timed intervals (30-40-50 s) to allow back-extrapolation to initial wet weights (16). Mucus samples were desiccated for more than 2 hours at 100°C, then reweighed to obtain dry weights and determine wet/dry ratios and percent solids.

Statistical Analyses

All data are expressed as mean ± SEM, unless otherwise specified. Paired Student's *t* test and one-way or two-way ANOVA followed by Bonferroni post-test were used to determine significant differences among groups. $P < 0.05$ was considered statistically significant and *n* represents the number of different donor lungs from which the cells were obtained.

RESULTS

Acute Apical Membrane Permeabilization with Nys Causes Na^+/K^+ATPase-Dependent Na^+ Hyperabsorption in Human Airway Epithelia

To characterize the acute effect of Nys on epithelial ion transport, we measured HBE bioelectric responses in Ussing chambers. Addition of Nys (40 μM) to the mucosal bath caused a large increase in I_{sc} (Figure 1A) and a decrease in R_T (Figure 1B). The increase in I_{sc} was transient and, after a progressive decline (~1 hour), I_{sc} returned approximately to basal levels (Figure 1A, *inset*, peak [A] and t > 200 min after challenge [B] values). The effect of Nys on I_{sc} was dose dependent, with the half-maximal activation (EC_{50}) in the range of 30 μM (Figure 1C). Although characterized by a common pattern (rapid increase, peak, gradual decrease), the profiles of Nys-induced I_{sc} varied among different cultures, even those derived from the same donor, perhaps reflecting differences in Nys insertion in the apical membrane.

To test whether the gradual decrease in I_{sc} could reflect inactivation/loss of Nys pores, we used a modified Ussing chamber that allows continuous perfusion of the mucosal surface. HBE cultures were exposed to pulses of fresh Nys alternating with KBR washing cycles (Figure 1D). After the first exposure to Nys, which induced a strong peak in I_{eq} followed by relaxation, the subsequent exposures failed to elicit a peak response of similar magnitude to the first exposure and produced progressively smaller I_{eq} peak responses. The I_{eq} responses to the subsequent Nys pulses, however, always exceeded baseline values. Notably, KBR washes appeared to quickly remove Nys pores from the mucosal surface, returning I_{eq} to pre-challenge baseline levels.

Based on the mechanism of action and ion selectivity of Nys pores, we hypothesized that the initial I_{sc} peak response was dominated by a Nys-induced intracellular Na^+ load that induced an increase in Na^+/K^+ATPase activity. To test whether the Nys-induced increase in I_{sc} was indeed carried by Na^+, we compared the response to acute Nys challenge in the presence or absence of Na^+ in the luminal bath, replacing Na^+ with N-methyl-D-glucamine (NMDG) before challenging the cultures with Nys. As shown in Figure 2A (representative tracings and summary bar graphs with average peak I_{sc} responses), Na^+ substitution significantly blocked the Nys-induced I_{sc} peak response.

Since NMDG is impermeable through the Nys pores and likely also has lower permeability than Na^+ through the paracellular pathway, replacement of Na^+ with NMDG alone might cause a decrease or reversal of the I_{sc} due both to limitation of cellular Na^+ entry and establishment of a bionic potential across the paracellular pathway (shunt current). To estimate the magnitude of the shunt current in the presence of NMDG in the apical chamber, we treated HBEs with amiloride (mucosal, 100 μM) to block the mucosal-to-serosal, transcellular Na^+ pathway (17, 18). Amiloride produced the expected decrease in I_{sc} (Figure 2B, *gray* and *black tracings*, ΔI_{sc} Amil in the bar graph). Upon Na^+ substitution with NMDG in the apical chamber (Figure 2B, *gray tracing*), we observed a further decrease in I_{sc} from the amiloride-treated values (ΔI_{sc} Amil/NMDG in the bar graph). This further decrease in I_{sc} likely reflects the larger serosal-to-mucosal Na^+ movement, compared to the mucosal-to-serosal NMDG movement, through the paracellular pathway (shunt current). Addition of Nys to amiloride-pretreated cultures in the presence of a normal Na^+ concentration (140 mM) in the mucosal bath produced a large increase in I_{sc} (Figure 2B, *black tracing*), whereas this increase in I_{sc} was substantially reduced when Nys challenge was

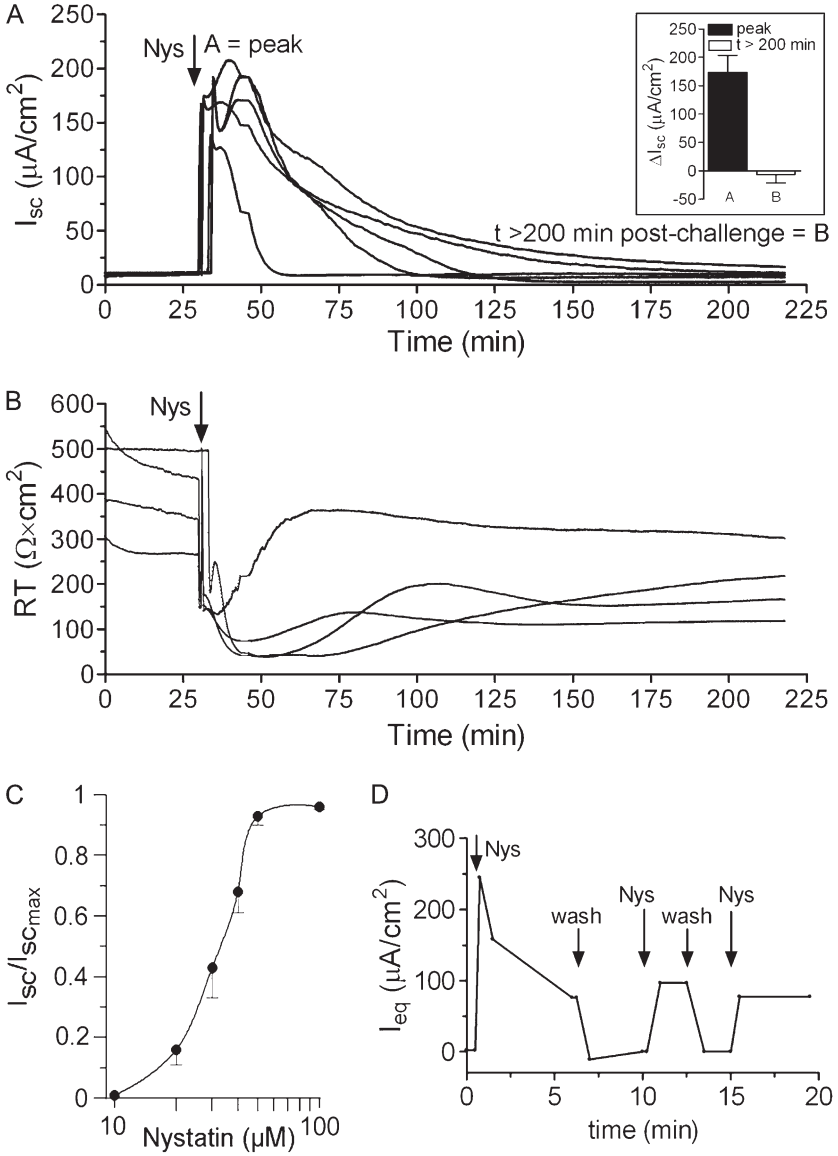

Figure 1. Acute Nys challenge causes a dose-dependent I_{sc} increase in primary HBE cells. (*A*) Representative Ussing chamber tracing illustrating the I_{sc} (*A*) and R_T (*B*) response of naïve HBEs to acute Nys challenge. *Inset* in *A*: *bar graph* showing average peak response (A) and t > 200 min after challenge values (B), mean ± SEM, $n = 11$. (*C*) Cumulative dose–response curve for the effect of Nys on I_{sc} in naïve HBEs. Data are shown as mean ± SEM, $n = 7$. (*D*) Representative tracing for measurements of I_{eq} in a modified perfusion Ussing chamber. *Arrows* indicate changes of the mucosal perfusate (Nys = 40 μM Nys in KBR, wash = KBR).

preceded by amiloride and Na^+ replacement with NMDG (Figure 2B, *gray tracing*). Because the I_{sc} response to NMDG after amiloride pretreatment (shunt current) was small (~ 7 μA/cm^2), the contribution of the shunt current to the large reduction in Nys-induced I_{sc} with mucosal amiloride/NMDG was small (compare the ΔI_{sc} Amil+Nys with the ΔI_{sc} Amil/NMDG+Nys, ~ 90 μA/cm^2). Moreover, the observation that amiloride pretreatment did not block the Nys peak response (compare ΔI_{sc} Amil+Nys in Figure 2B with ΔI_{sc} KBR+Nys in Figure 2A) suggests that Nys creates an ENaC-independent, unregulated path for Na^+ entry as expected based on Nys' mechanism of action.

To test whether the Nys-induced I_{sc} was dependent on the activity of the basolateral Na^+/K^+ATPase, we tested the effect of ouabain (1 mM, serosal), a specific inhibitor of the Na^+/K^+ATPase, on the I_{sc} response elicited by acute Nys challenge. As shown in Figure 2C, pretreatment with ouabain significantly blunted the Nys-induced increase in I_{sc}, demonstrating that the Nys-induced I_{sc} response required the activity of the Na^+/K^+ATPase.

Next, we explored the possibility that the Nys-induced increase in I_{sc} was due to serosal-to-mucosal anion movement. We tested the effect of blocking Cl^- transport on the Nys-induced I_{sc} peak response by inhibiting Cl^- entry through the Na-K-2Cl cotransporter (NKCC), located in the basolateral membrane of airway epithelial cells, with bumetanide (100 μM). As shown in Figure 3A, inhibition of Cl^- entry did not significantly inhibit the Nys-induced I_{sc} peak response, consistent with the notion that the Nys-induced ΔI_{sc} predominantly reflected increased Na^+ absorption.

We also tested the effect of acute Nys challenge on HBE bioelectrics in the complete absence of Cl^- on both sides of the epithelium. The Nys peak was significantly blunted in bilateral Cl^--free KBR as compared to bilateral KBR conditions (Figure 3B). Although it is possible that a portion of the I_{sc} peak response to Nys is due to Cl^- secretion, the striking discrepancy between the absence of a bumetanide effect on Nys peak response and the inhibition of the Nys response by complete removal of Cl^- might be explained by the analysis of the effect of Cl^- substitution on the electrochemical driving force for Na^+ entry. Based on previous studies (19), removal of Cl^- from the apical compartment would significantly depolarize the apical membrane (e.g., reduction of luminal Cl^- to 3 mM depolarized the apical membrane $\Delta V_a + 12.1$ mV). Further, bilateral Cl^- substitution is predicted to induce cell shrinkage and a consequent increase in intracellular

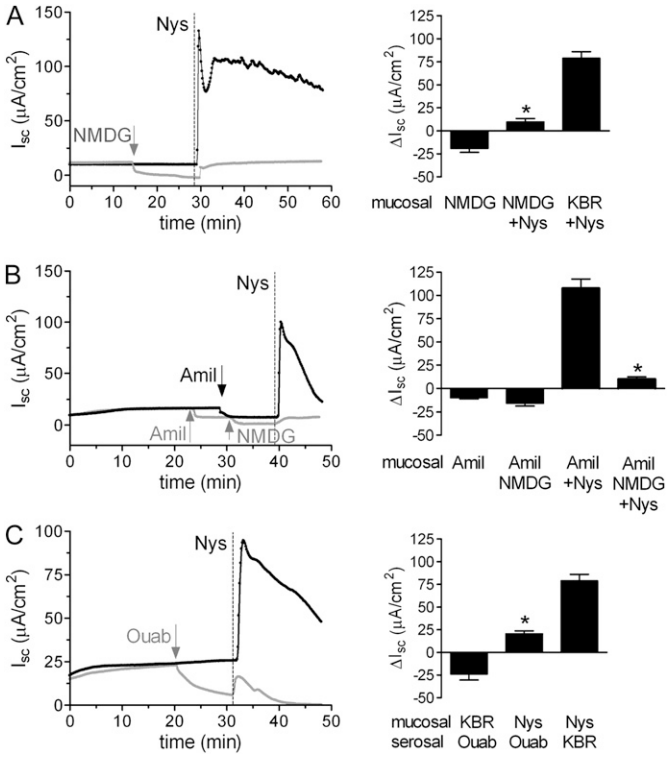

Figure 2. Acute Nys challenge causes Na^+ hyperabsorption in primary HBE cells. (*A*) Representative Ussing chamber tracings illustrating the I_{sc} response of naïve HBEs to acute Nys challenge (Nys, *vertical dashed line*) after Na^+ replacement (mucosal NMDG, *gray tracing*) or without Na^+ replacement (*black tracing*). Compiled data from the experiment depicted in *A* are shown in the *bar graph* as mean ± SEM, $n = 3$ individual donors, 3 to 4 cultures/condition; $^*P < 0.0001$ versus KBR+Nys. (*B*) Representative Ussing chamber tracings illustrating the I_{sc} response to acute Nys challenge (Nys, *vertical dashed line*) of HBEs pretreated with amiloride (Amil, mucosal) and subjected or not to Na^+ replacement with NMDG (*gray* and *black tracing*, respectively). Compiled data from the experiment depicted in *B* are shown in the *bar graph* as mean ± SEM, $n = 3$ individual donors, 3 to 4 cultures/condition; $^*P < 0.0001$ versus Amil+Nys. (*C*) Representative Ussing chamber tracings illustrating the I_{sc} response to acute addition of Nys (Nys, *vertical dashed line*) in ouabain-treated (Ouab, *gray tracing*) and untreated HBEs (*black tracing*). Compiled data from the experiments depicted in *C* are shown in the *bar graph* as mean ± SEM, $n = 3$ individual donors, 3 to 4 cultures/condition; $^*P < 0.0001$ versus Nys/KBR. Average peak I_{sc} responses to Nys are shown in all the *bar graphs*.

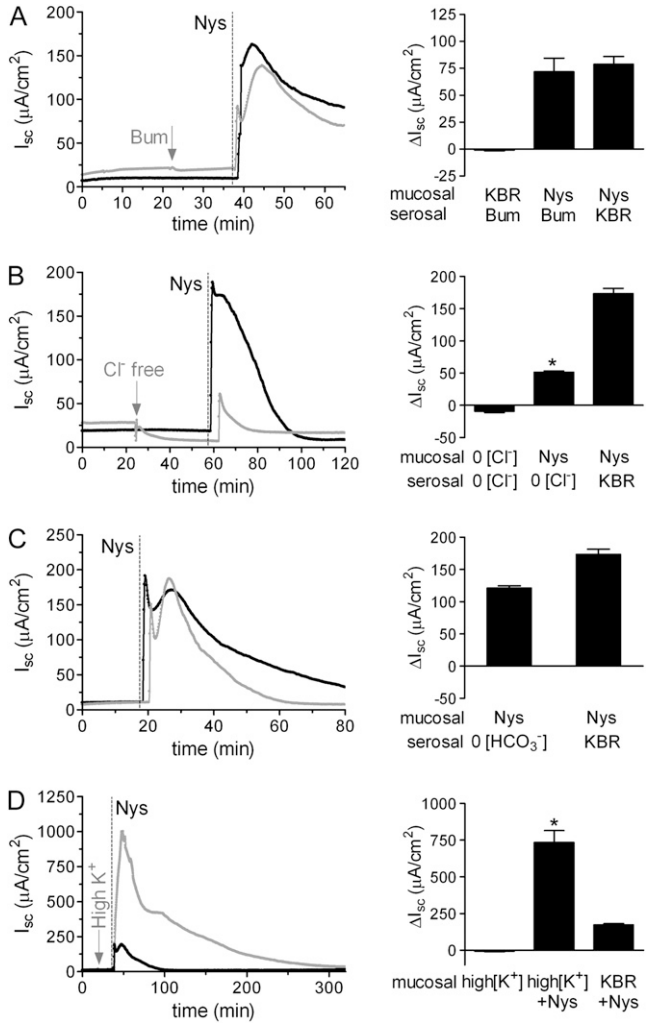

Figure 3. Contribution of Cl^-, HCO_3^-, and K^+ to the response of HBEs to acute Nys treatment. Representative Ussing chamber tracings illustrating the I_{sc} response to acute Nys challenge (Nys, *dashed line*) in bumetanide-treated (*A*, Bum, *gray tracing*); bilateral Cl^- free KBR (*B*, Cl^- free, *gray tracing*); bilateral HCO_3^- free KBR (*C*, HCO_3^- free, *gray tracing*); and mucosal high K^+ KBR (*D*, high K^+, *gray tracing*) compared with untreated HBEs (*black tracing*). Compiled data from the experiments depicted in all panels are shown in the *bar graph* as mean ± SEM, $n = 2$ to 3 individual donors, 4 to 6 cultures/condition. $^*P < 0.0001$ versus Nys/KBR. Average peak I_{sc} responses to Nys are shown in all the *bar graph*.

Na^+ activity. Thus it is likely that bilateral Cl^- substitution reduced the I_{sc} response to Nys because the electrochemical driving force for Na^+ entry was substantially reduced by the Cl^- substitution maneuver.

To exclude the participation of other relevant anions in the acute Nys peak response, we performed challenges in the absence of HCO_3^-. We observed peak responses equivalent to those measured in the presence of HCO_3^- (Figure 3C).

Interestingly, when HBEs mucosally bathed in high K^+ KBR were challenged with Nys, the peak response was strikingly enhanced (Figure 3D). These data suggest that when K^+ efflux through the Nys pores is prevented by elevation of the luminal $[K^+]$, the absolute magnitude of net Na^+ influx is revealed. As previously reported, elevation of the extracellular $[K^+]$ did not affect HBE bioelectrics in the absence of Nys (20).

Taken together, these data demonstrate that mucosal application of Nys to HBEs induces predominantly Na^+ absorption that is dependent on Nys concentration and Na^+/K^+ATPase. However, as another measure of the net ion transport triggered by Nys, we measured luminal liquid volume transport.

Acute Nys Challenge Promotes Mucosal Volume Absorption

In airway epithelia, transepithelial Na^+ transport constitutes the driving force for liquid absorption from the luminal compartment. To test whether Na^+ hyperabsorption induced by acute Nys challenge was coupled to an increased mucosal volume absorption by HBEs, we performed thin film measurements of ASL volume absorption using live cell confocal imaging, as previously described (12). Figure 4A shows representative images taken in the XZ scanning mode after establishment of thin-film conditions (ASL volume ~ 1 μl) on naïve HBEs in the absence or presence of Nys (HBSS and HBSS+Nys, t = 0), and after 1 hour of incubation in a highly humidified incubator (t = 1 h). In the absence of Nys, we observed ASL heights in the 7 μm range, as expected for

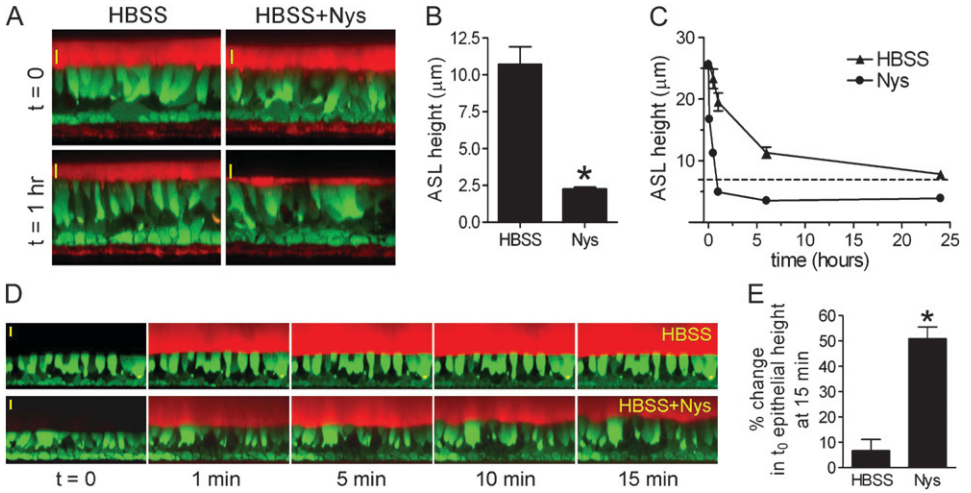

Figure 4. Acute Nys challenge promotes mucosal volume absorption in HBEs and induces cell swelling in the presence of large mucosal volume. (*A*) Representative XZ confocal images of HBEs loaded with Calcein-AM (*green signal*) and layered with Texas Red–labeled ASL volume (thin film conditions, *red signal*) in the absence (HBSS) or presence of Nys (HBSS+Nys), at t = 0 (*upper panels*) and t = 1 hour of incubation in highly humidified incubator (*lower panels*). *Scale bar* = 10 μm. (*B*) Compiled data from thin film measurements of steady state ASL volume. Data are expressed as ASL height and shown as mean ± SEM, $n = 4$ individual donors, 2 cultures/condition; *$P < 0.0001$. (*C*) Kinetic measurements of ASL volume absorption by naïve HBEs in the absence (HBSS) or presence of Nys (Nys). (*D*) Representative sequence of XZ confocal images of calcein-loaded naive HBEs used for cell swelling measurements upon acute Nys challenge in the presence of large mucosal volume. At t = 1 minute, 200 μl of Texas Red–labeled HBSS (*upper panel*) or HBSS+Nys (*lower panel*) were mucosally applied. *Scale bar* = 10 μm. (*E*) Compiled data for epithelial cell swelling measured as increase in epithelial height over baseline (t = 0) at 15 minutes. Data are shown as average ± SEM, $n = 3$ individual donors, 2 cultures/condition; *$P < 0.01$ versus HBSS.

normal HBEs. In contrast, the presence of Nys in the mucosal liquid significantly increased the volume absorptive capacity of HBEs. Importantly, as shown in Figure 4B, in the presence of Nys the steady-state ASL height dropped well below 7 μm, the physiologic threshold previously shown to be essential for maintaining proper ciliary beating and mucus clearance (2). Thus, Nys produces an apical Na^+ channel that is not appropriately regulated (inhibited) at low ASL volumes.

To define the volume absorption kinetics of HBEs in the presence and absence of mucosal Nys, 10 μl of Texas Red dextran-labeled volume with or without Nys were layered on the mucosal surface of the cultures and imaged at serial time points (5 min, 30 min, 1 h, 6 h, and 24 h). Figure 4C shows that Nys promoted a faster rate of volume absorption (~5 μm/min in the absence of Nys compared with ~20 μm/min in the presence of Nys) that significantly reduced ASL height below the 7 μm threshold (*dashed line*). This reduction persisted throughout the 24-hour observation period. Collectively, these data indicate that Nys both accelerates the rate of volume absorption and bypasses the physiologic inhibition of Na^+ absorption at low ASL volumes.

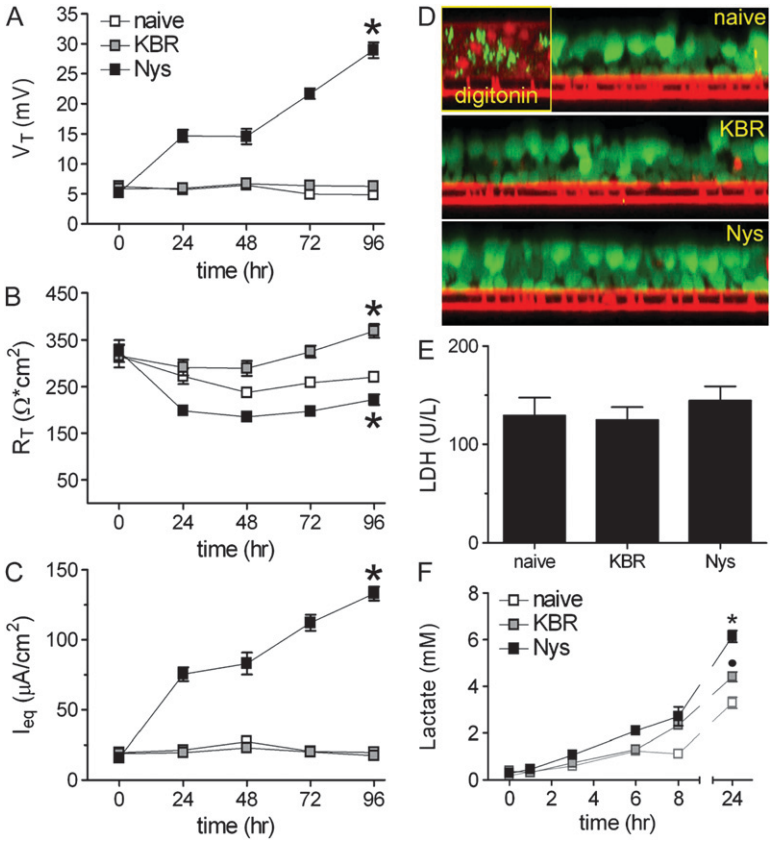

Figure 5. Chronic mucosal Nys treatment promotes sustained Na^+ hyperabsorption in airway epithelial cells in the absence of cell toxicity. (*A–C*) EVOM measurements of HBEs bioelectric properties in naïve, KBR-, and Nys-treated cultures. (*A*) transepithelial voltage (V_T); (*B*) transepithelial resistance (R_T); and (*C*) calculated equivalent current (I_{eq}). Data are shown as mean ± SEM, $n = 6$ individual donors, 2 to 4 cultures for each treatment, *$P < 0.001$ significantly different vs. naïve cultures. (*D*) Representative images illustrating the absence of ethidium homodimer-1 staining (marker of cell death) in naïve, KBR-, and Nys- treated cells subjected to the DEAD/LIVE cell fluorescence assay. Positive control = digitonin-treated HBEs. (*E*) Lactate dehydrogenase (LDH) activity in the basolateral media of naïve, KBR-, and Nys-treated cultures after 96 hours of Nys treatment. Data are shown as mean ± SEM, $n = 3$ individual donors, 2 cultures for each treatment. (*F*) Time-course of lactate accumulation in the serosal media of naïve, KBR-, and Nys-treated cultures. Data are shown as mean ± SEM, $n = 4$ individual donors, 2 cultures for each treatment; *$P < 0.001$ Nys versus naïve and KBR-treated cultures, •$P < 0.001$ KBR versus naïve cultures.

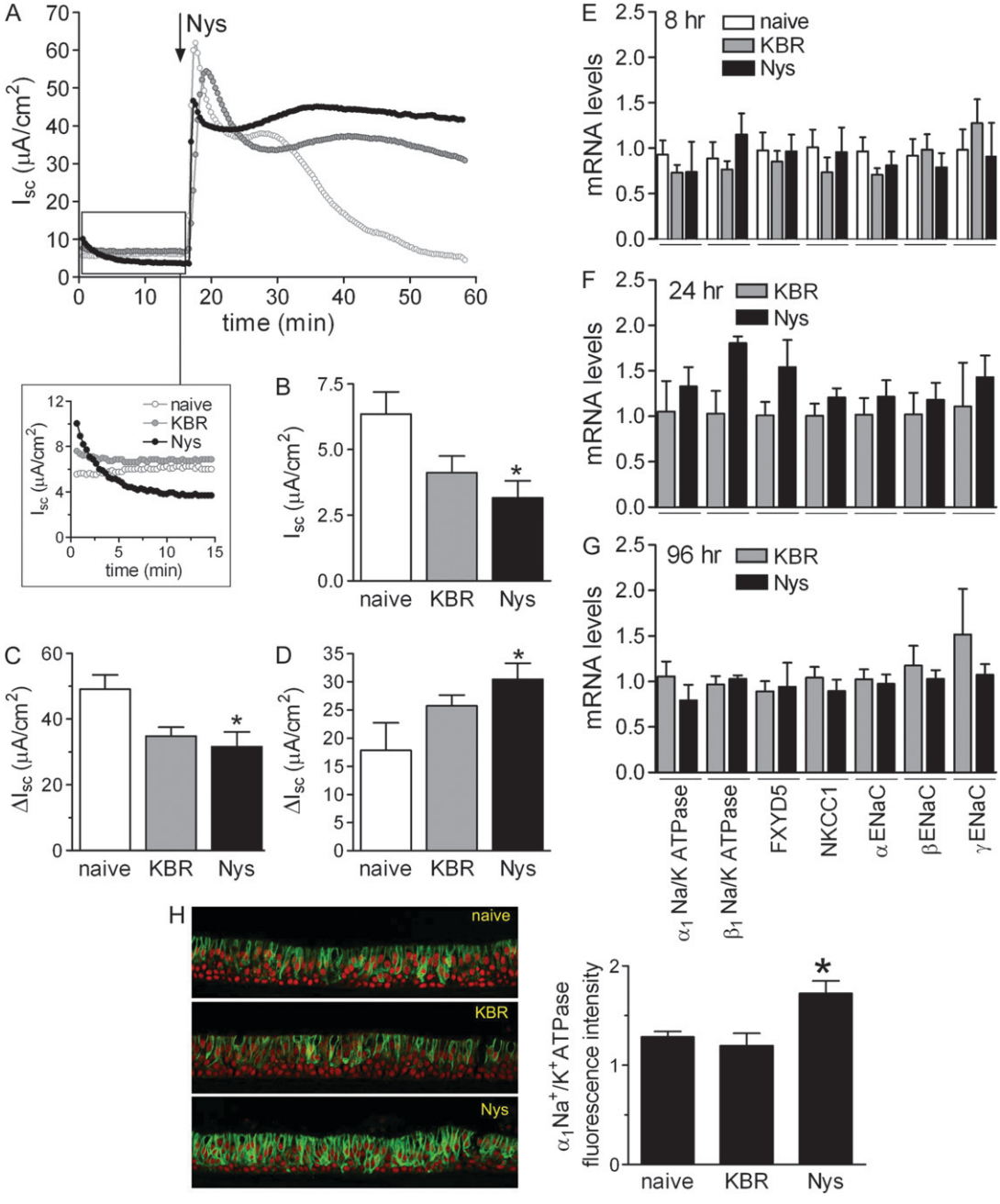

Figure 6. Chronic mucosal Nys treatment does not affect the bioelectric properties of primary HBE cells nor total mRNA abundance of transepithelial Na^+ transport mediators. (*A*) Representative Ussing chamber tracings showing the effect of chronic Nys and KBR treatment on I_{sc}. The enlarged panel shows the rapid loss (completed in ~ 15 min) of chronic Nys effect (e.g., increased I_{sc}) upon mounting of the cultures in a Nys-free mucosal bath. (*B*) Baseline I_{sc} values 15 minutes after mounting naïve, KBR-, and Nys-treated culture in the chambers (data are shown as mean ± SD, $n = 4$ individual donors, 4 to 6 cultures for each treatment; $^*P = 0.01$ versus naïve cultures). The *arrow* in Figure 1A indicates the acute addition of Nys in the apical chamber. (*C*) ΔI_{sc} between peak value after acute Nys addition and baseline value (peak-basal); (*D*) ΔI_{sc} value between the I_{sc} value at 40 minutes and baseline value and (40min-basal). Data are expressed as mean ± SEM, $n = 4$ individual donors, 4 to 6 cultures for each treatment; $^*P < 0.05$ versus naïve cultures. (*E*) Quantitative RT-PCR analysis of epithelial Na^+ transport path components in naïve, KBR-, and Nys-treated cultures after 8 hours of treatment. Similar data were obtained at (*F*) 24 hours and (*G*) 96 hours of treatment. Data are shown as mean ± SEM, $n = 2$ individual donors, 4 cultures for each treatment. (*H*) Representative confocal images of naïve, KBR-, and Nys-treated HBE cultures immunostained for α_1 Na^+/K^+ATPase. Quantification of the $\alpha_1 Na^+/K^+$ATPase-specific signal is shown in the *bar graph* as mean ± SEM, $n = 3$ individual donors, 2 cultures for each treatment. $^*P < 0.05$ significantly different versus naïve and KBR-treated cultures.

Acute Nys Challenge in the Presence of Large Mucosal Volume Causes Cell Swelling

The initial uncontrolled intracellular Na^+ load elicited by Nys permeabilization of the apical cell membrane is predicted to promote cell swelling if a large volume of liquid is present on the mucosal surface. To study changes in cell volume, we performed real time imaging of calcein-loaded HBEs after applying to the apical surface 100 to 200 μl of liquid to the apical surface in the presence or absence of Nys. As shown in Figure 4D, addition of Nys in a large mucosal volume induced a gradual and significant cell swelling as compared with HBEs exposed to the same volume load without Nys (HBSS). In the presence of Nys, the epithelial height reached a plateau in approximately 15 minutes and the cells remained swollen for over 45 minutes (data not shown). The percentage change in t_0 epithelial height at 15 minutes, in the absence or presence of Nys, is depicted in Figure 4E. Previous studies have shown that mucosal addition of amphotericin B increased the intracellular Na^+ activity from 23 to 65 mM, with bioelectric changes similar to those induced by Nys (7). Thus, HBE cell swelling in the presence of a large mucosal volume is consistent with a Nys-induced increase in intracellular NaCl, followed by osmotically driven water influx. Although we could not assess whether volume absorption was taking place over the 45-minute period of observation (ASL height exceeded the objective working distance), the data shown in Figures 5A and 7A below indicate that acute cell swelling in

the presence of large mucosal volume did not affect epithelial integrity or prevent mucosal volume absorption.

Chronic Mucosal Nys Treatment Promotes Sustained Na^+ Hyperabsorption in Airway Epithelial Cells

To mimic more closely the chronic Na^+ hyperabsorption present in CF airway epithelia, we next evaluated the effect of chronic Nys treatment (40 μM mucosal Nys for 4 d) on HBEs by comparing the bioelectric properties (measured by EVOM voltohmeter during the treatment, as described in MATERIALS AND METHODS) of Nys-treated cultures with both nontreated (naïve) and vehicle (KBR)-treated cultures. As shown in Figure 5A, chronic mucosal Nys treatment increased V_T over time, whereas naïve or KBR-treated cultures exhibited no change in V_T. After 96 hours of treatment, Nys-treated cultures exhibited a lower R_T compared to naïve cultures, whereas in KBR-treated cultures we observed a slight increase of R_T in comparison to naïve cultures (Figure 5B). Of note, after the first 24 hours of treatment, Nys-treated cultures maintained steady R_T values of approximately 200 $\Omega \cdot cm^2$ for 4 days, indicating that epithelial integrity was preserved. The equivalent current (I_{eq}) of Nys-treated cultures was significantly increased over time compared to naïve and KBR-treated cultures (Figure 5C). After 4 days of Nys treatment, I_{eq} values reached a plateau (data not shown).

Chronic Mucosal Nys Treatment Is Not Toxic for Airway Epithelial Cells

To test *in situ* whether Nys treatment affected the viability of HBEs, we performed a cell-based assay using fluorescent probes that distinguish between live (calcein-positive, *green fluorescence*) and dead (ethidium homodimer-1–positive, *red fluorescence*) cells. We found no evidence that chronic Nys treatment was toxic for HBEs, whereas dead cells were clearly identified in the positive control, that is, digitonin-treated cells (Figure 5D). We next assessed whether chronic Nys treatment had a cytotoxic effect by measuring lactate dehydrogenase (LDH) activity in the serosal medium from naïve, KBR-, and Nys-treated cultures after 96 hours of treatment. As shown in Figure 5E, no difference in LDH levels among the different conditions was detected.

Chronic Mucosal Nys Treatment Increases Serosal Lactate Secretion by Airway Epithelial Cells

We noticed that, during chronic Nys treatment, KBR- and Nys-treated cultures tended to acidify the basolateral media (indicated by a shift toward yellow in phenol red–containing media) more rapidly than naïve cultures. We speculated that the higher transepithelial Na^+ transport induced by Nys was coupled to increased energy expenditure. Since primary epithelial cells in prolonged culture conditions usually rely on glycolytic metabolism (21), we performed time courses for the accumulation of lactate (the end product of the glycolytic metabolism) in the serosal media of naïve, KBR-, and Nys-treated cultures. As shown in Figure 5F, 24-hour lactate accumulation after 96 hours of treatment was higher in Nys- than either KBR-treated or naïve cultures, whereas the lactate levels of KBR-treated cultures were intermediate between naïve and Nys-treated cultures. These data suggest that Nys- and, to a lesser extent, KBR-treated cultures exhibited a higher metabolic energy demand, likely associated with increased Na^+ transport/volume load.

Chronic Mucosal Nys Treatment Does Not Permanently Change the Bioelectric Properties of Airway Epithelial Cells

We next tested whether chronic Nys treatment would permanently affect the bioelectric properties of HBEs as measured in Ussing chambers. The representative tracings shown in Figure 6A were recorded immediately after mounting in the chambers cultures chronically treated for 96 hours. We found that the Nys-induced increase in I_{sc} (illustrated in Figure 5C) waned within 5 minutes after the culture was bathed in bilateral KBR (*see* Figure 6A, *inset*). These data suggest that, even after prolonged treatment, Nys binding to the apical membrane was weak, and it was rapidly reversible when Nys was diluted more than 40-fold in the mucosal bath. These findings are in agreement with the perfusion chamber experiment shown in Figure 1D.

After establishment of the new baseline ($\sim$ 15 min), chronically Nys-treated cultures exhibited baseline I_{sc} values slightly lower than those of naïve cultures (*see* representative tracings in the inset of Figure 6A and the *bar graph* with average baseline I_{sc} values in Figure 6B). All cultures responded to a second Nys challenge with a rapid increase in I_{sc}, and the average peak values for Nys-pretreated cultures were slightly smaller than those of naïve cultures (Figure 6.C). Altogether, these data suggest that chronic Nys treatment did not grossly modify the basal activity of the Na^+ pump in HBE cells.

Interestingly, for naïve cells, the Nys-induced peak in I_{sc} was followed by a gradual decrease as previously shown (Figure 1A), whereas for Nys- and KBR-pretreated cultures the Nys-induced I_{sc} was generally sustained for longer times, as indicated by the ΔI_{sc} after 40 minutes in comparison to naïve cultures (Figure 6D). This latter finding suggests that although the chronic treatment (both with KBR or Nys) did not alter the ability of the transepithelial Na^+ transport system to respond to an acute Na^+ load, it did modify the long-term response of HBEs to this stimulus. Given the absence of dramatic differences in baseline I_{sc} and Nys-induced peak I_{sc} values among naïve, chronically KBR–treated, and chronically Nys–treated cultures and considered the high variability of late-phase profiles normally obtained upon acute Nys challenge, we did not further explore the etiology of this long-term post-Nys challenge response.

Chronic Mucosal Nys Treatment Does Not Affect mRNA Abundance of Key Elements of the Transepithelial Na^+ Transport Path

To assess directly whether chronic Nys treatment modulated the mRNA abundance of key elements of the transepithelial Na^+ transport path, we performed quantitative RT-PCR analysis on total mRNA extracted from naïve, KBR-, and Nys-treated cultures at 8, 24, and 96 hours. We evaluated mRNA expression of the following genes: the catalytic $\alpha_1 Na^+/K^+$ATPase subunit; the $\beta_1 Na^+/K^+$ATPase subunit; FXYD5, a newly identified modulator of the Na^+/K^+ATPase activity, particularly abundant in epithelial cells from kidney, intestine, and lung (22); the basolateral Na-K-2Cl cotransporter (NKCC1); and the three subunits of the epithelial Na^+ channel, i.e., α-, β-, and γ-ENaC. As shown in Figure 6E, no significant differences were detected in the mRNA abundance among naïve, KBR-, and Nys-treated cultures after 8 hours of treatment. We obtained similar results for later time points (e.g., 24 and 96 h [Figures 6F and 6G]), suggesting that Nys treatment did not affect the mRNA abundance of the major components of the Na^+ transport system.

To investigate one aspect of ion transport element regulation at the protein level, we performed immunofluorescence localization studies of the $\alpha_1 Na^+/K^+$ATPase subunit. The immunolocalization pattern in cultured HBE cells (Figure 6H) was in agreement with the basolateral expression expected for the Na^+/K^+ATPase in airway epithelia (23). Similarly to what has been reported for primary cultures of human nasal epithelial cells chronically exposed to the polyene antibiotic Amphotericin B (AmphoB) (23), chronic Nys treatment did not perturb the

basolateral localization of the Na^+/K^+ATPase. However, quantification of the α_1Na^+/K^+ATPase-specific fluorescence signal in naïve, KBR-, and Nys-treated cultures after 96 hours of treatment revealed a slight but significant increase in the expression of the α_1Na^+/K^+ATPase in Nys-treated compared with naïve cultures (Figure 6H), in contrast with chronic AmphoB treatment, which was found to reduce the expression and activity of the Na^+ pump.

Chronic Nys Treatment Promotes Sustained Mucosal Volume Absorption in Airway Epithelial Cells

HBE cultures chronically treated with Nys or KBR exhibited striking differences in the rates of absorption of the fluid applied on their mucosal surfaces. The rate of mucosal volume absorption was quantified by collecting the fluid remaining on the mucosal surface at 8- and 16-hour intervals after the application of KBR or Nys in 120 μl KBR, throughout the chronic treatment protocol. As shown in Figure 7A, Nys-treated cultures showed a significant increase in the rate of volume absorption within the first 8 hours of treatment (9 μl/h with Nys versus 3 μl/h without Nys). The volume absorption rates increased slightly after the first 8 hours of treatment and did not change significantly thereafter (16 μl/h versus 9 μl/h, 15 μl/h versus 6 μl/h, 14 μl/h versus 6 μl/h, and 15 μl/h versus 7 μl/h, in the presence versus absence of Nys, at 16, 24, 48, and 72 h, respectively). These data are in agreement with the findings from Figure 4C, suggesting that Nys promotes liquid absorption soon after initiation of the treatment. Figure 7B shows representative images of the mucosal surfaces of naïve, KBR-, and Nys-treated cultures after 4 days of chronic treatment. Whereas KBR-treated cultures still had liquid on their surface, Nys-treated cultures appeared completely dry. Moreover, as illustrated by the *arrowheads* in Figure 7B, lumps of what appears to be mucosal secretions could be seen at the cell surface of KBR-treated cultures, mostly confined at the periphery of the cell culture. Similarly, in naïve culture the periphery of the culture is where most of the mucosal secretions tend to accumulate over time, likely due to the centrifugal motion of coordinated cilia beating (not shown). In contrast, mucosal secretions and cell debris were plastered to the entire cell surface of Nys-treated cultures, forming macroscopic string-like aggregates.

Chronic Mucosal Nys Treatment Leads to Mucus Dehydration/Compaction over Airway Epithelial Cells

We investigated at the microscopic level the mucosal surfaces of naïve, KBR-, and Nys-treated cultures after 4 days of chronic Nys treatment (Figure 7B) by performing OsO_4/perfluorocarbon fixation to preserve the mucus and periciliary layers as previously reported (2, 24). As shown in Figure 8A (*left panels*), both naïve and KBR-treated cultures exhibited ASL height of approximately 7 μm, with freely extended cilia. In contrast, Nys-treated cultures exhibited a depletion of periciliary liquid with "bent" cilia and had a thick layer of dense material adherent to the cell surface.

To assay for the presence of mucopolysaccharides in this thick layer, we performed Alcian Blue–Periodic Acid Schiff (AB-PAS) staining on 4% paraformaldehyde–fixed cultures. This staining revealed that the dense material on Nys-treated cultures contained mucinous substances (Figure 8A, *right panels*). Of note, Nys treatment did not appear to stimulate intracellular accumulation of AB-PAS–positive mucous substances in HBEs (Figure 8A, *right panels*).

As shown in Figure 8A, after 4 days of treatment the mucous layer is only about 10 μm thick. Because of the small volume, we could not collect samples of this material to determine its level of hydration after 4 days. Therefore, we prolonged the treatment (decreasing the amount of applied fluid to 50 μl, and the frequency of volume challenge to once a day to prevent prolonged periods of flooding and hypoxia in KBR-treated cultures) until we could visually identify masses of mucous material on the surface of naïve, KBR-, and Nys-treated cultures (i.e., 14 d). We then collected these secretions, measured the wet/dry ratio, and calculated the percentage of solids as indices of dehydration. As shown in Figure 8B, the percentage of solids of the mucous material sampled from the surface of Nys-treated cultures exceeded those of naïve and KBR-treated cultures, indicating that such material was markedly dehydrated.

DISCUSSION

In the present study, we sought to model the dysregulated Na^+ absorptive phenotype of CF airway epithelia in primary cultures of normal bronchial epithelial cells with acute and chronic mucosal Nys treatment.

To characterize our model, we first studied the bioelectric response of HBEs to acute Nys challenge. We found that acute Nys challenge in primary HBEs produced a dose-dependent, rapid increase in I_{sc} followed by a gradual relaxation of the response (Figure 1A). Diverse responses to acute Nys challenge in Ussing chambers have been described in the literature. Although a pattern similar to the one we observed has been described in toad bladder A6 cells and rat colonic epithelium (13, 25), other model systems (e.g., Calu-3 cells) responded to acute Nys exposure with a slower rise in I_{sc} (10–20 min) and a plateau phase that was sustained for over 30 minutes (26, 27). Since Nys binding to the plasma membrane is strictly dependent on sterol content (28), these differences might be attributed to differences in the apical membrane sterol composition in the different cell types studied.

Detailed characterization using ion substitution and specific inhibitors of ion transport revealed that the acute bioelectric response of HBE to Nys challenge reflected multiple ion transport responses, with Na^+ absorption being the dominant one. The initial, steep increase in I_{sc} was dependent on the presence of Na^+ in the luminal bath (Figures 2A and 2B) and on the activity of the basolateral Na^+/K^+ATPase (Figure 2C). The failure of amiloride pretreatment to inhibit the Nys-induced I_{sc} peak (Figure 2B) suggested that Nys challenge elicits ENaC-independent Na^+ absorption.

Nys-induced I_{sc} was not affected by bumetanide (Figure 3A) or $HCO3^-$ substitution (Figure 3C). However, there was a significant blunting of this response by bilateral removal of Cl^- (Figure 3B). These results suggest that either Cl^- secretion was a component of the I_{sc} response or that Cl^- substitution had an adverse effect on the electrochemical gradient for Na^+ entry across the apical membrane. The former possibility seems unlikely for three reasons. First, previous patch clamp studies showed that Nys forms pores that have a small, finite Cl^- permeability only when used at high concentrations (150–400 μM) (9). In dog bronchial epithelial cells, mucosal Nys increased the Cl^- permeability across the apical membrane only at concentrations higher than 90 μM (29). Lower concentrations of Nys (50 μM), comparable to the one used in our studies, have been shown to selectively affect Na^+ transport in immortalized Calu-3 human airway epithelial cells (26). Second, the Nys-induced I_{sc} was insensitive to bumetanide (Figure 3A). Third, the possibility that Cl^- secretion was a component of the I_{sc} response of HBE to acute Nys challenge is inconsistent with our data showing that Nys treatment enhanced the volume absorptive properties of HBE both acutely and chronically (Figures 4A–4C and 7A).

We could also detect evidence of K^+ secretion concurrent with Na^+ absorption upon acute Nys treatment (Figure 3D). However, a greater net rate of Na^+ absorption dominated, as evidenced by the polarity of the I_{sc} response and the liquid absorption measurements. In agreement with this notion, acute

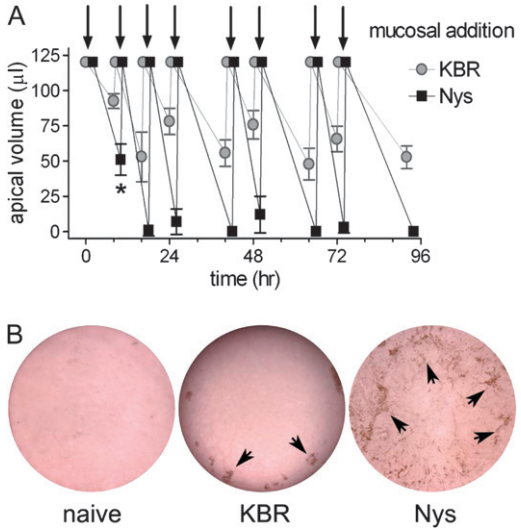

Figure 7. Chronic mucosal Nys treatment leads to sustained mucosal volume absorption. (*A*) Macroscopic determination of mucosal volume absorption. 120 μl of either KBR or KBR+Nys were mucosally applied to the cultures (*arrows*) according to the chronic Nys treatment protocol. Mucosal liquid volume was estimated every 8 and 16 hours. Data are shown as mean ± SD, $n = 4$ individual donors, 2 cultures for each treatment; *$P = 0.018$, 8 hours versus 24 hours time point in Nys-treated cultures. (*B*) Representative images of the surface of naïve, KBR-, and Nys-treated cultures after 96 hours chronic Nys treatment. KBR-culture surface is out of focus for the presence of mucosal liquid on top of the culture. Note the mucus and cellular debris accumulating towards the periphery of the cultures in KBR-treated cultures whereas firmly adherent to the cell surface in Nys-treated cultures (*arrowheads*).

Nys administration produced cell swelling (Figure 4D), consistent with cellular accumulation of Na^+ ions and H_2O, whereas an increase in K^+ secretion is predicted to produce cell shrinkage. Cell swelling was not observed in thin film conditions (Figure 4A), suggesting that Na^+ influx through Nys pores, followed by osmotically driven H_2O influx, requested large luminal volumes to produce cell swelling. Also note that the Nys-induced swelling was restricted to the luminal columnar cell layer, whereas the basal cell layer appeared to be unaffected, suggesting that Nys pores were confined to the apical membrane of the "mucosal" cell layer (Figure 4D).

In agreement with a previous study (30), we showed that acute Nys-dependent Na^+ hyperabsorption was coupled to a rapid increase in the rate of mucosal fluid absorption (Figures 4A and 4B). More importantly, the data shown in Figure 4C suggest that Nys can reproduce both the Na^+ transport and the ASL volume regulation defects associated with CF. Specifically, cultures exposed to Nys exhibited more rapid initial rate of volume absorption, consistent with an accelerated rate of Na^+ absorption. Moreover, Nys-treated cultures were unable to inhibit volume absorption as the ASL volume approached the critical 7 μm threshold required for efficient ciliary beating and mucus transport. This latter defect (i.e., failure to inhibit ENaC at low ASL volume) may be the most critical defect in the Na^+ transport path in CF (31) and appears to be mimicked by Nys. In CF the failure to regulate ENaC at low ASL volume reflects the absence of functional CFTR (1). With Nys, the absence of Na^+/volume absorption regulation likely reflects the inability of endogenous regulators of ENaC to inhibit Nys pores (30). Regardless of mechanistic differences, Nys appears to model both features of dysregulated Na^+ transport exhibited by CF airway epithelia.

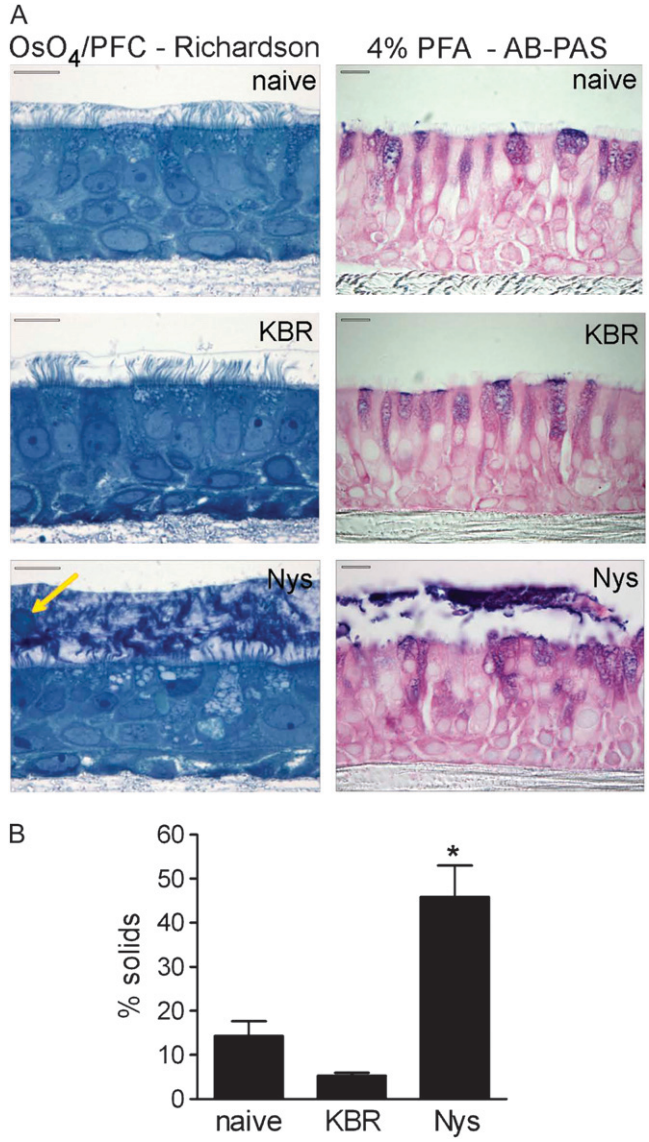

Figure 8. Chronic mucosal Nys treatment causes mucus dehydration and adherence to the cell surface of primary HBE cells. (*A*) Representative images of naïve, KBR-, and Nys-treated cultures fixed with OsO_4/PFC and stained with Richardson's staining (*left panels*) or fixed with 4% PFA and stained with AB-PAS for detection of mucin molecules (*right panels*). Note the thick layer of dense material at the surface of Nys-treated culture, with embedded cellular debris (*arrow*). AB-PAS *blue* and *magenta stain* in the intra- and extra-cellular compartments indicates the presence of acid and neutral mucins, respectively. *Scale bar* = 10 μm. (*B*) Percent solids content of plugs isolated from the cell surface of naïve, KBR-, and Nys-treated cultures after long-term (i.e., 14 d) treatment (data are shown as mean ± SD, $n = 4$ individual donors, 2 cultures for each treatment; *$P = 0.001$ versus naïve and KBR-treated cultures).

To study the effect of chronic apical membrane permeabilization, we treated HBE cultures with 40 μM Nys for 4 days. In the experimental design for the chronic Nys treatment, we considered two conditions to control for the volume of liquid and mass of NaCl applied to the Nys-treated cultures, that is, non–volume-treated (naïve, 0 μl) and volume-treated (KBR, 120 μl) cultures compared with Nys/volume-treated (Nys+KBR, 120 μl) cultures. We showed that chronic Nys treatment significantly increased V_T and I_{eq} over time, while affecting R_T only at early time points

(Figures 5A–5C) compared with either control, suggesting that the functional integrity of the epithelia was preserved.

Transcellular Na^+ transport driven by the basolateral Na^+/K^+ATPase is an energy-consuming process. Although we found no signs of overt cytotoxicity induced by the chronic Nys treatment (Figures 5D and 5E), we observed increased levels of lactate in the serosal media of KBR- and Nys-treated cultures, suggesting that both conditions imposed an increased energy demand on HBE cultures (Figure 5F). We speculate that Nys-treated cultures faced the highest metabolic energy expenditure as a consequence of the increased Na^+ transport due the increased Na^+ permeability in the apical membrane after insertion of Nys pores. In the case of the KBR-treated cultures, the increase in lactate concentration in comparison to naïve cultures could reflect the hypoxic conditions created by the continuous presence of liquid on the mucosal surface of these cultures. Alternatively, the higher metabolic energy demand could reflect an increase in Na^+ transport due to the persistent high activation state of ENaC elicited in airway epithelia by the dilution of ENaC inhibitory factors normally present in the ASL (30, 32).

A recent study has shown that chronic mucosal treatment of normal nasal epithelial cells with 50 μM amphotericin B (AmphoB) significantly reduced V_T, I_{sc}, and amiloride-sensitive I_{sc} (23). AmphoB treatment did not affect cellular metabolism or integrity, but decreased expression of αENaC, α_1Na^+/K^+ATPase, and NKCC1. These findings were interpreted to result from a feedback mechanism aimed to limit cellular Na^+ overload due to membrane permeabilization with AmphoB. In contrast, our data indicate that Nys produced a sustained increase in I_{sc} (Figures 5A–5C) coupled to increased volume absorption (Figure 7A) without significant effects on the expression of major components of transcellular Na^+ transport system (Figures 6E–6H). In the same experimental conditions used in our study, acute AmphoB challenge caused a rapid increase in I_{sc} similar to the one elicited by acute Nys (*see* Figure E1A in the online supplement). Although both Nys and AmphoB belong to the polyene antibiotic family and, at least acutely, have similar effects on the bioelectric properties of airway epithelial cells, a comparison between our results and those of Jornot and coworkers (23) suggests that the different outcomes might be dependent on the different interactions of AmphoB versus Nys with the plasma membrane. For example, our data showed that Nys binding to the plasma membrane was rapidly reversible, and even after chronic exposure the bioelectric properties of Nys-treated cultures after significant Nys dilution, were comparable to those of naïve HBEs. In contrast, AmphoB interactions with the plasma membrane are likely stronger, since the time required to recover normal bioelectric properties depends on the duration of the AmphoB-exposure (23), regardless of the removal of the drug from the mucosal solution. Due to the rapid reversibility of the induced hyperabsorptive phenotype, Nys could be the reagent of choice when secondary modification of the bioelectric properties of the cultures or long recovery time after treatment are unwanted.

Importantly, during the chronic Nys treatment protocol, we observed a striking difference in ASL volume homeostasis between KBR- and Nys-treated cultures that persisted over 4 days (Figure 7A). The persistence of this hyperabsorptive response over 4 days suggests that long-term Nys treatment produced a sustained increase in HBE Na^+ transport. Consistent with short-term ASL volume experiments in which the mucus layer was removed from the cell surface (Figures 4A–4C), we found that after 4 days of chronic Nys treatment, the PCL was depleted and the cilia were not fully extended (Figure 8A, *left panels*). In contrast, naïve and KBR-treated cultures exhibited a normal ASL phenotype, with the cilia outstretched in an approximately 7-μm high periciliary layer. Further, the cilia and the apical surface of Nys-treated cultures were covered with a thick layer of condensed, strongly AB-PAS–positive material (Figure 8A, *right panels*). This phenotype strongly resembles the appearance of mucus-plugged CF airways (33). It is worth stressing that our ability to still detect the mucous material on the cell surface of Nys-treated cultures after the repeated washings required for 4% PFA fixation indicates that the interaction between the condensed layer and the epithelial surface was strong.

Assessment of the percentage of solids of mucus plaques collected after long-term Nys treatment quantitatively showed that the material lining the surface of Nys-treated cultures was dehydrated compared with that harvested from naïve or KBR-treated cultures (Figure 7B). In humans, mucus from bronchiectatic individuals ranges from 4 to 8% solids, whereas CF mucus ranges from 11 to 20% solids (34). The "% solids" values measured for the material lining the Nys-treated cultures were higher than those noted in CF HBE cultures after 3 days in culture (24) or in CF lungs *in vivo*. The higher value could reflect the presence of dead cells in the plugs, as evident in the histologic sections where cell debris entrapped in the mucus layer can be easily seen (Figure 8A, and Figure E1B in the online supplement). Overall, chronic Nys treatment did not appear to promote goblet cell hyperplasia in HBEs. Nevertheless, at this point we can not rule out the possibility that chronic Nys treatment also promoted mucin hypersecretion, perhaps through activation of voltage-sensitive Ca^{2+} channels (35), compounding the effect of dehydration in the accumulation of concentrated mucus at the mucosal surface.

In conclusion, we have shown that Nys treatment of normal primary airway epithelial cells recapitulates two key features characterizing CF airway epithelia: (*1*) abnormal Na^+ transport, as reflected by both accelerated rate of Na^+ absorption and, most critically, failure to regulate Na^+ absorption at low ASL volume, producing ASL volume depletion on airway surfaces; and (*2*) accumulation of dehydrated, "thickened" mucous material that adheres to the cell surface. The Nys model presents some advantages in comparison to cultured CF HBEs. Besides being inexpensive and readily available, Nys treatment is not influenced by culture conditions and it is applicable to a wide variety of cultured cells, for example, tracheal and bronchial primary, passage 1 and passage 2 cells, primary nasal cells, and mouse tracheal cells. However, the Nys model also suffers from limitations. First, the lack of selectivity on cation transport by Nys pores, (i.e., the parallel increase in K^+ as well as Na^+ permeability) does not strictly model the CF defect. Second, Nys treatment may exert a subtle pro-inflammatory action on airway epithelial cells (36) of different nature as the inflammation observed in CF airways. Third, although we provided evidence of lack of cytotoxicity, the details about how HBE cells respond to long-term intracellular Na^+ load are still unknown. Despite these potential limitations, this simple *in vitro* model that features luminal thickened mucus may be useful for characterizing the interactions of bacteria, inflammatory cells, and soluble factors in a CF-like luminal milieu. Potentially, this model may also be used to study the adhesive interaction between mucus layers and airway epithelial surface, providing data on the mechanisms involved in mucus adherence and, hence, clues as to novel therapies for CF lung disease.

Conflict of Interest Statement: None of the authors has a financial relationship with a commercial entity that has an interest in the subject of this manuscript.

Acknowledgments: The authors thank: Dr. Scott Randell at the UNC CF Center Tissue Core for providing the HBE cells; Kimberly Burns and Tracy Eldred at the UNC CF Center Histology Core; Dr. Michael Chua and Wendy Salmon for the invaluable help at the UNC Michael Hooker Microscopy Facility; Drs. Jack Stutts and Sheriff Gabriel for making available the Ussing Chambers setup; Troy Rogers for performing the lactate determination; and Rodney Gilmore in the Molecular Biology Core for technical assistance with LightCycler quantitative RT-PCR assay.

References

1. Tarran R, Button B, Picher M, Paradiso AM, Ribeiro CM, Lazarowski ER, Zhang L, Collins PL, Pickles RJ, Fredberg JJ, *et al.* Normal and cystic fibrosis airway surface liquid homeostasis: the effects of phasic shear stress and viral infections. *J Biol Chem* 2005;280:35751–35759.
2. Matsui H, Grubb BR, Tarran R, Randell SH, Gatzy JT, Davis CW, Boucher RC. Evidence for periciliary liquid layer depletion, not abnormal ion composition, in the pathogenesis of cystic fibrosis airways disease. *Cell* 1998;95:1005–1015.
3. Boucher RC. Evidence for airway surface dehydration as the initiating event in CF airway disease. *J Intern Med* 2007;261:5–16.
4. Mall M, Grubb BR, Harkema JR, O'Neal WK, Boucher RC. Increased airway epithelial Na^+ absorption produces cystic fibrosis-like lung disease in mice. *Nat Med* 2004;10:487–493.
5. Randell SH, Walstad L, Schwab UE, Grubb BR, Yankaskas JR. Isolation and culture of airway epithelial cells from chronically infected human lungs. *In Vitro Cell Dev Biol Anim* 2001;37:480–489.
6. Willumsen NJ, Boucher RC. Transcellular sodium transport in cultured cystic fibrosis human nasal epithelium. *Am J Physiol* 1991;261:C332–C341.
7. Willumsen NJ, Boucher RC. Sodium transport and intracellular sodium activity in cultured human nasal epithelium. *Am J Physiol* 1991;261:C319–C331.
8. Ribeiro CM, Paradiso AM, Carew MA, Shears SB, Boucher RC. Cystic fibrosis airway epithelial Ca_i^{2+} signaling: the mechanism for the larger agonist-mediated Ca_i^{2+} signals in human cystic fibrosis airway epithelia. *J Biol Chem* 2005;280:10202–10209.
9. Horn R, Marty A. Muscarinic activation of ionic currents measured by a new whole-cell recording method. *J Gen Physiol* 1988;92:145–159.
10. Fulcher ML, Gabriel S, Burns KA, Yankaskas JR, Randell SH. Well-differentiated human airway epithelial cell cultures. *Methods Mol Med* 2005;107:183–206.
11. Paradiso AM, Ribeiro CM, Boucher RC. Polarized signaling via purinoceptors in normal and cystic fibrosis airway epithelia. *J Gen Physiol* 2001;117:53–67.
12. Tarran R, Boucher RC. Thin-film measurements of airway surface liquid volume/composition and mucus transport rates in vitro. *Methods Mol Med* 2002;70:479–492.
13. Rokaw MD, Sarac E, Lechman E, West M, Angeski J, Johnson JP, Zeidel ML. Chronic regulation of transepithelial Na^+ transport by the rate of apical Na^+ entry. *Am J Physiol* 1996;270:C600–C607.
14. Sims DE, Westfall JA, Kiorpes AL, Horne MM. Preservation of tracheal mucus by nonaqueous fixative. *Biotech Histochem* 1991;66:173–180.
15. Sheehan D, Hrapchak B. Theory and practice of histotechnology. Columbus, Ohio: Battelle Press; 1980.
16. Knowles MR, Robinson JM, Wood RE, Pue CA, Mentz WM, Wager GC, Gatzy JT, Boucher RC. Ion composition of airway surface liquid of patients with cystic fibrosis as compared with normal and disease-control subjects. *J Clin Invest* 1997;100:2588–2595.
17. Knowles MR, Stutts MJ, Spock A, Fischer N, Gatzy JT, Boucher RC. Abnormal ion permeation through cystic fibrosis respiratory epithelium. *Science* 1983;221:1067–1070.
18. Knowles M, Murray G, Shallal J, Askin F, Ranga V, Gatzy J, Boucher R. Bioelectric properties and ion flow across excised human bronchi. *J Appl Physiol* 1984;56:868–877.
19. Willumsen NJ, Davis CW, Boucher RC. Intracellular Cl^- activity and cellular Cl^- pathways in cultured human airway epithelium. *Am J Physiol* 1989;256:C1033–C1044.
20. Willumsen NJ, Davis CW, Boucher RC. Cellular Cl^- transport in cultured cystic fibrosis airway epithelium. *Am J Physiol* 1989;256:C1045–C1053.
21. Harris SI, Balaban RS, Barrett L, Mandel LJ. Mitochondrial respiratory capacity and Na^+- and K^+-dependent adenosine triphosphatase-mediated ion transport in the intact renal cell. *J Biol Chem* 1981;256:10319–10328.
22. Lubarski I, Pihakaski-Maunsbach K, Karlish SJ, Maunsbach AB, Garty H. Interaction with the Na,K-ATPase and tissue distribution of FXYD5 (related to ion channel). *J Biol Chem* 2005;280:37717–37724.
23. Jornot L, Rochat T, Caruso A, Lacroix JS. Effects of amphotericin b on ion transport proteins in airway epithelial cells. *J Cell Physiol* 2005;204:859–870.
24. Tarran R, Grubb BR, Parsons D, Picher M, Hirsh AJ, Davis CW, Boucher RC. The CF salt controversy: In vivo observations and therapeutic approaches. *Mol Cell* 2001;8:149–158.
25. Schultheiss G, Lan Kocks S, Diener M. Stimulation of colonic anion secretion by monochloramine: Action sites. *Pflugers Arch* 2005;449:553–563.
26. Ito Y, Nakayama S, Son M, Kume H, Yamaki K. Protection by tetracyclines against ion transport disruption caused by nystatin in human airway epithelial cells. *Toxicol Appl Pharmacol* 2001;177:232–237.
27. Son M, Ito Y, Sato S, Ishikawa T, Kondo M, Nakayama S, Shimokata K, Kume H. Apical and basolateral ATP-induced anion secretion in polarized human airway epithelia. *Am J Respir Cell Mol Biol* 2004;30:411–419.
28. Coutinho A, Silva L, Fedorov A, Prieto M. Cholesterol and ergosterol influence nystatin surface aggregation: Relation to pore formation. *Biophys J* 2004;87:3264–3276.
29. Haas M, McBrayer DG. Na-K-Cl cotransport in nystatin-treated tracheal cells: regulation by isoproterenol, apical utp, and [cl]i. *Am J Physiol Cell Physiol* 1994;266:C1440–C1452.
30. Tarran R, Trout L, Donaldson SH, Boucher RC. Soluble mediators, not cilia, determine airway surface liquid volume in normal and cystic fibrosis superficial airway epithelia. *J Gen Physiol* 2006;127:591–604.
31. Button B, Picher M, Boucher RC. Differential effects of cyclic and constant stress on ATP release and mucociliary transport by human airway epithelia. *J Physiol* 2007;580:577–592.
32. Kunzelmann K, Schreiber R, Cook D. Mechanisms for the inhibition of amiloride-sensitive Na^+ absorption by extracellular nucleotides in mouse trachea. *Pflugers Arch* 2002;444:220–226.
33. Livraghi A, Randell SH. Cystic fibrosis and other respiratory diseases of impaired mucus clearance. *Toxicol Pathol* 2007;35:116–129.
34. Chernick WS, Barbero GJ. Composition of tracheobronchial secretions in cystic fibrosis of the pancreas and bronchiectasis. *Pediatrics* 1959;24:739–745.
35. Boitano S, Woodruff ML, Dirksen ER. Evidence for voltage-sensitive, calcium-conducting channels in airway epithelial cells. *Am J Physiol* 1995;269:C1547–C1556.
36. Razonable RR, Henault M, Watson HL, Paya CV. Nystatin induces secretion of interleukin (IL)-1beta, IL-8, and tumor necrosis factor alpha by a toll-like receptor-dependent mechanism. *Antimicrob Agents Chemother* 2005;49:3546–3549.